Finite Element Based Multi-Objective Design Optimization Procedure of Interior Permanent Magnet Synchronous Motors for Wide Constant-Power Region Operation

F. Parasiliti, M. Villani, S. Lucidi, F. Rinaldi

***Abstract* – The paper proposes a design optimization procedure of three-phase Interior Permanent Magnet synchronous motors with minimum weight, maximum power output and suitable for wide constant-power region operation. The particular rotor geometry of the Interior Permanent Magnet synchronous motor and the presence of several variables and constraints make the design problem very complicated. Authors propose to combine an accurate Finite Element analysis with a multi-objective optimization procedure using a new algorithm belonging to the class of Controlled Random Search algorithms.**

The optimization procedure has been employed to design two Interior Permanent Magnet motors for industrial application and city electrical scooter. A prototype has been realized and tested: comparison between predicted and measured performance shows the reliability of the simulation results and the effectiveness, the versatility and the robustness of the proposed procedure.

***Index Terms*—Permanent magnet motors, design optimization, search methods, finite element methods, automotive applications, design methodology, electric vehicles, flux-weakening, magnetic analysis, variable speed drives.**

NOMENCLATURE

d–q	Rotating reference frame.
v_d, v_q	d–q stator voltage components.
i_d, i_q	d–q stator current components.
Φ_M	Stator flux linkage amplitude due to the magnet.
ω	Electrical speed.
R	Stator phase resistance.
L_d, L_q	d–q stator synchronous inductances.
T	Electromagnetic torque.
p	Number of pole pairs.
x	Design variables.
$f(x)$	Objective function.
$g(x)$	Constraint functions.
l, u	Variables lower and upper limits.
F	Variables feasible set.
$P(x)$	Augmented objective function.
n	Number of design variables.
k	Iteration index.
S^k	Set of points chosen at random.
m	Number of points in S^k.
L_S	Losses per radiating slot surface.
σ	Current density.
k_s	Stator slot fill factor.
ρ	Copper resistivity.
w_s	Average slot width.
h_s	Slot high.
γ	Angle between current vector and q-axis.

Manuscript received December 23, 2010. Accepted for publication June 18, 2011.

F. Parasiliti and M. Villani are with the Department of Electrical and Information Engineering, University of L'Aquila, Italy (e-mail: francesco.parasiliti@univaq.it; marco.villani@univaq.it)).

S. Lucidi and F. Rinaldi are with the Department of Computer and System Sciences "Antonio Ruberti", "Sapienza" University of Rome, Italy. (e-mail: lucidi@dis.uniroma1.it; rinaldi@dis.uniroma1.it).

I. INTRODUCTION

The Interior Permanent Magnet (IPM) synchronous motors, built with magnets placed inside the rotor body, are attracting great attention in several variable speed applications, such as electric vehicles, industrial and domestic appliances, where the most challenging requirements are high efficiency, high torque density, good overload capability and extended speed range.

Additional features are the robustness of the rotor structure, mechanically suited to high speed operation, and the presence of magnetic saliency: the "direct" d-axis inductance is substantially different from the "quadrature" q-axis inductance, where the d-axis is aligned with the Permanent Magnet (PM) flux according to the equivalent Park model of the synchronous machine. This characteristic is particularly suited for extending the torque/speed operating region by proper "field weakening" control techniques: the most popular approach is to combine the maximum torque per ampere trajectory with the voltage-constraint-tracking field-weakening control [1]-[5]; moreover, it allows the application of some interesting approaches to position and speed detection, namely "self-sensing" or "sensorless" control [6]-[8].

On the other hand, IPM motors have quite strong non-linear operating characteristics, often increased by saturation and

mutual axes interaction ("cross-coupling") [9].

Then, to take advantage of the motor features, during design stage performance prediction should be reliable all over the operating range. The accurate analysis of these motors requires the use of numerical techniques like Finite Element (FE) method that takes into account the remarkable saturation phenomena in certain parts of the rotor especially if magnets are fully buried and enclosed by the rotor core. Reference [10] shows the use of FE method to calculate the torque, reluctance torque, back iron flux density, tooth flux density, detent torque, and back electromotive force of IPM motors. In [11] an IPM motor was designed by using an equivalent magnetic circuit model where inductance and iron-loss resistance, which are affected critically by magnetic saturation, are obtained by using FE analysis. In [12] the conventional *d,q*-axes mathematical model was modified in order to include data derived from three-dimensional finite element analysis (FEA). Indirect interaction between FEA and circuit simulation enhances model fidelity embodying the influence of saturation and cross-coupling effects.

Moreover, the demand of high-performance motors needs the use of design optimization procedure in combination with suitable analytical or FE motor models: that is the most popular approach to design IPM motors in literature. Differences concern the motor model, the aim of the optimization, the design object (part or all the motor), the requirement of an initial feasible design and the search method.

In [13] novel rotor designs of IPM motors in order to reduce harmonic iron losses at high rotational speeds under field-weakening control were proposed: an optimization method, combined with an adaptive FE method, was applied to automatically determine the shapes of the magnets and rotor core.

Two case studies were proposed in [14]. In the first, the goal of the optimization was to obtain a back-emf with a maximal amplitude and low distortion. A coupled FE-grid-search algorithm was implemented in order to synthesize the shape of the rotor surface with only one design variable, the radius of the rotor surface. In the second, a multiobjective rotor topology optimization has been presented, coupling FE calculations with genetic algorithms. The chosen objective functions were the amplitude of the phase flux linkage first harmonic and the reciprocal value of the cogging torque amplitude. The same authors in [15] proposed a multiobjective optimization design method using three different optimization algorithms (Hooke-Jeeves, genetic algorithms, and grid-search). The optimizations were performed in two stages: the Hooke-Jeeves and genetic algorithms methods were used for the global search and a fine grid-search was done around the optimum given by the first two methods. The efficiency and the cost of the active materials and technology were considered as fitness functions. The multiobjective optimization was performed using an analytical model with embedded FE correction factors. Seven design variables were considered. Methods to reduce acoustic noise in an interior permanent-magnet motor during the design stage have been presented in [16]. In [17] a method was proposed to design the optimal stator configurations of a traction motor of hybrid electric vehicle to reduce torque ripples. The focus of the paper in [18] was to improve the self-sensing performance of an interior permanent-magnet synchronous machine (IPMSM) by modifying the rotor configurations. A finite element analysis has been used to design and assess the performance of the machine for self-sensing. In [19] the rotor design was discussed in order to reduce the estimation error caused by cross-saturation in the sensorless control.

The objective to improve the flux-weakening capability of IPM motors find a wide interest in the literature. In [20] analytical models were used and validated by FE computations. The design was formulated as a constrained multiobjective optimization problem consisting of maximizing the machine efficiency while minimizing its weight. At the end of the process the designer made a posteriori choice. Reference [21] analyzed by FE simulations how to maximize the performance modifying the PM quantity. Reference [22] proposed rotor design optimization of IPM motors for wide speed ranges by means of a FEA-based multi-objective genetic algorithm with 3 goal functions (motor torque, torque ripple and flux weakening capability).

This paper proposes a design optimization procedure of three-phase Interior Permanent Magnet synchronous motors suitable for wide constant-power region operation with the aim to minimize the motor weight and maximize the output power.

Peculiarities of the proposed approach are the following:

- the objective function is multiple (three), one term conflicting with the others;
- the optimization is performed in two distinct operating points (rated and high speed);
- the design concerns all the motor (stator and rotor core, winding and magnets);
- some of the design variables vary in a discrete way with fixed steps;
- all motor performance are evaluated by FE method;
- the design procedure does not need to start from a known initial design, i.e. a feasible initial design is not required.

The proposed design optimization of IPM motors is based on a new algorithm belonging to the class of Controlled Random Search (CRS) algorithms that derives from the algorithm proposed in [23]. CRS algorithms follow a strategy which combines a global search phase and a local search phase. The proposed Finite Element based multi-objective optimization procedure is employed to design two machines with different rotor structures: a single-barrier, 6 pole motor for industrial application (Fig. 1a) and a double-barriers, 4 pole motor for city electrical scooter (Fig.1b).

The conventional single-layer IPM model is the simplest solution, with a significant reduction on the manufacturing cost respect to the double-layer one. The second solution is popular in the recent years since its high saliency ratio rotor structure benefits to increase the machine performance and the torque quality.

a) b)

Fig. 1. Typical cross sections of the considered IPM motors (1 pole).

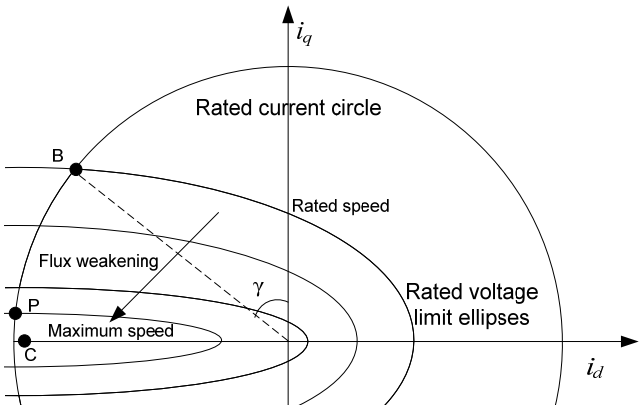

Fig. 2. Constant voltage and current loci in the *d-q* currents plane.

II. Motor Basic Representations

The steady-state IPM motor stator voltage equations written in the *d-q* rotating reference frame are:

$$v_d = R\,i_d - \omega L_q\,i_q \qquad 1)$$

$$v_q = R\,i_q + \omega L_d\,i_d + \omega \Phi_M \qquad 2)$$

where:

i_d , i_q , v_d and v_q are the d and q axis components of the armature current and terminal voltage respectively, R is the winding resistance per phase, L_d and L_q are the axis inductances, ω is the electrical speed and Φ_M is the magnets flux linked with the d axis armature winding.

The electromagnetic torque is calculated using the well known equation:

$$T = \frac{3}{2}\,p\left[\Phi_M\,i_q + \left(L_d - L_q\right)i_d\,i_q\right] \qquad 3)$$

where p is the number of pole pairs.

Simple manipulations of the basic relations (1-3) provide the basic expressions of the constant voltage and current loci in the *d-q* currents plane, respectively represented by "voltage ellipse" and "current circle" (Fig. 2). At rated condition they share a point which is the "rated" operating point of the IPM motor (point B); for increasing speed (and fixed rated voltage) one has a family of voltage "limit" ellipses which converge to their center (point C): in that point the speed is theoretically infinite and the torque is zero.

Above base speed, the operation is limited by the rated current and the rated voltage and the motor is controlled by the "field-weakening" method. The operating points under these limit conditions are the intersections between the current limit circle and the voltage limit ellipses, and the current vector moves from B to P, where the speed is maximum. Since the constant voltage constraint, the flux decreases and hence the torque, in inverse proportion to speed.

III. The Design Approach

To guarantee a wide constant power operation, the motor requires an accurate design through use of salient rotor geometry with limited flux contribution from PMs buried within the rotor structure. To achieve the desired degree of saliency, maximize the power density and guarantee good performance, special lamination profile should be found.

The particular rotor geometry of the IPM synchronous motor and the presence of several variables and constraints make the design problem very complicated to solve. A good way is to carry out a design procedure, combining accurate FE analysis with mathematical optimization algorithms: the paper proposes a new design approach based on this idea.

The study concerns the design of the following two IPM synchronous motors:

- a 5 kW, 6 poles, 36 slots motor for industrial application (M1 motor). The chosen rotor presents one barrier per pole and the magnet material is inserted into this cavity.
- a 4 kW, 4 pole, 36 slots motor for city-electrical-scooter (M2 motor): the rotor presents two magnet layers per pole, a choice that provides higher saliency ratio than the single-layer design. The design constraints are in compliance with a conventional 100 cc scooter for 2 passengers with a rated speed of 30 km/h and maximum speed of 70 km/h.

The choice of different number of barriers results from the applications and costs. IPM synchronous motor guarantees high torque generation at constant current and wide speed operating range if the q-axis inductance is high [24], [25]. This can be obtained, for a constant magnet volume, by splitting up each rotor pole in two (or more) PM cavity layers with iron separation in the radial direction in order to increase the anisotropy in the magnetic path, and thereby enhancing the saliency. However, the addition of one more cavity increases the complexity in the rotor construction and its manufacturing cost.

The stator and rotor consist of a stack of laminated high permeability non-oriented grain silicon steel: 330-50 AP and 330-35 AP for M1 and M2 respectively. Three-phase double-layer distributed windings are inserted in the stator slots. NdFeB magnets are chosen due to their high energy density: remanent flux density B_r at 20°C is 1.16 T and the coercive field strength H_c is 900 kA/m.

A temperature of 90°C is considered for the stator windings and 75°C for the PMs. These values have been chosen taking into account the cooling systems of the considered machines: liquid cooled for M1 and air-forced cooled for M2. These efficient systems allows to guarantee a maximum operating temperature in the stator windings usually below 80÷90 °C.

The IPM synchronous motors are modelled using FE "parametric models" that allow to vary the geometric dimension of motor, the current distribution and rotor position. Torque prediction is carried out for several stator-rotor relative positions and the finite element grid is automatically adjusted when the rotor is rotated. The influence of mesh has been investigated in order to get satisfactory accuracy avoiding the inaccuracies due to the element distortion. Only one pole is simulated, due to the motor symmetries.

The input data of the FE model are the motor geometry and the *d-q* axis currents. By means of an out-of-line procedure, the phase currents are assigned to each slot. The motor torque is calculated by Virtual Work principle.

The qualitative aim of the optimization is to maximize the torque at the base and high speeds, extending the flux weakening region and minimizing the motor weight. The aim is pursued by a multi-objective optimization procedure with the following objectives:

a) maximize the torque at base speed (point B, Fig. 2);
b) maximize the torque at maximum speed (point P, Fig. 2);
c) minimize the weight of the motor.

The optimization is performed in the operating points B and P corresponding to the values shown in Table I.

Voltage values are chosen according to the applications. Currents amplitude and vector angle γ are defined on the base of a preliminary study [26]. In B, speed is calculated on the base of voltage, current and angle values; in P, speed depends on the optimization because it is "constrained" to be higher than a chosen value (see Table IV), i.e. as higher as possible (maximum).

TABLE I
OPERATING POINTS

Motor			M1	M2
	Rated voltage	V	150	44
	Rated current	A	30	90
Point B (base speed)	Current vector angle γ	deg.	35	45
	Speed	rpm	4000	2600
Point P (high speed)	Current vector angle γ	deg.	85	80
	Speed	It depends on the optimization		

The design variables concern the stator and rotor core, the PM size and the stator winding. The rotor shape should be designed in order to have, in addition to the PM torque, a torque component due to the anisotropy of the rotor: an accurate design of the flux barriers can increase the difference between the reluctance of *d*–axis and *q*–axis, increasing the reluctance torque component and improving the motor performance when it is driven at constant power over a wide speed range.

The set of variables $\boldsymbol{x}$ used in the optimization procedure are listed in Table II and Table III, with their limits, and shown in Fig. 3 and Fig. 4.

The limits on the design variables have been chosen in order to guarantee the feasibility of the final designs. The wide ranges of these "box constraints" and the high number of variables and constraints make the optimization problem very complicated and could require significant computational effort, but allow to define in detail a reliable final design.

The design M1 has 18 variables: among these, 6 variables (stack length, outer stator diameter, number of wires per slot, wire size and flux barriers angles) vary in discrete way.

The design M2 has 16 variables: among these, 5 variables (stack length, number of wires per slot, wire size and flux barriers angles) vary in discrete way. The outer stator diameter is fixed according to the available space for the motor housing inside the scooter.

TABLE II
DESIGN M1: MINIMUM AND MAXIMUM RANGES OF DESIGN VARIABLES

Discrete variables		min	max	step
x1. Stack length	mm	60	90	1
x2. Outer stator diameter	mm	100	130	1
x14. Angle of flux barrier	deg.	-10	10	1
x15. Angle of flux barrier	deg.	-10	10	1
x17. Number of wires per slot		4	14	1
x18. Wire size	mm	1.0	2.0	0.05
Continuous variables		min	max	-
x3. Inner stator diameter	mm	72	80	-
x4. Stator tooth width	mm	2.0	3.0	-
x5. Stator yoke thickness	mm	3.0	5.0	-
x6. Slot opening width	mm	1.2	1.6	-
x7. Slot opening depth	mm	1.0	2.0	-
x8. Bottom loop radius	mm	0.3	0.8	-
x9. Upper loop radius	mm	0.3	0.8	-
x10. PM thickness	mm	2.0	4.0	-
x11. Ratio of PM width to barrier width		0.80	0.95	-
x12. Magnet position	mm	4.0	8.0	-
x13. Rotor tooth width	mm	4.0	6.0	-
x16. Thickness of steel bridge	mm	2.0	3.0	-

TABLE III
DESIGN M2: MINIMUM AND MAXIMUM RANGES OF DESIGN VARIABLES

Discrete variables		min	max	step
x1. Stack length	mm	90	130	1
x13. Angle of flux barrier	deg.	-10	10	1
x14. Angle of flux barrier	deg.	-10	10	1
x15. Number of wires per slot		1	10	1
x16. Wire size	mm	1.0	5.0	0.05
Continuous variables		min	max	-
x2. Stator tooth width	mm	2.5	5.0	-
x3. Stator yoke thickness	mm	4.0	10.0	-
x4. Slot opening width	mm	1.5	2.5	-
x5. Inner PM position	mm	6.0	12.0	-
x6. Inner PM thickness	mm	2.0	8.0	-
x7. Distance between PMs	mm	2.0	10.0	-
x8. Outer PM thickness	mm	2.0	5.0	-
x9. Ratio of inner PM width to barr. width		0.8	0.95	-
x10. Ratio of outer PM width to barr. width		0.8	0.95	-
x11. Thickness of steel bridge	mm	1.0	3.0	-
x12. Rotor tooth width	mm	5.0	15.0	-

In this study, fixed steps have been chosen for the discrete variables, but in a manufacturing environment, these increments can be varied according to normalized values (particularly for the stack length, outer diameter and wire size). For good electromagnetic performance, it should be necessary to minimize the steel bridges surrounding the magnetic cavities. On the other hand the centrifugal force on steel bridges should be taken into account, being the dominant source of mechanical stress in high speed operation. From a preliminary analysis a minimum value of 2 mm has been

imposed for M1 and 1 mm for M2: these values are consistent with the maximum speed and mechanical stress.

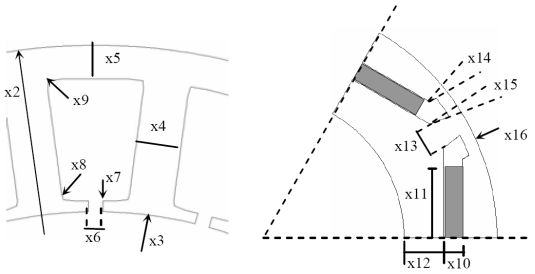

Fig. 3. Design M1 – Variables

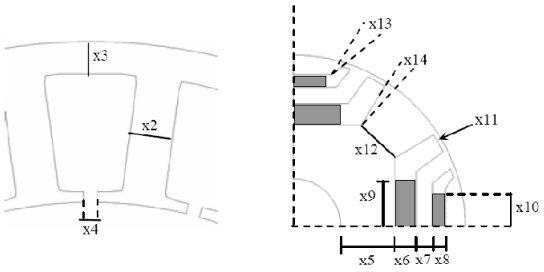

Fig. 4. Design M2 – Variables

TABLE IV
CONSTRAINTS

Constraints		M1	M2
c1. Stator slot fill factor		≤ 0.40	≤ 0.40
c2. Max flux density in the stator tooth	T	≤ 1.80	≤ 1.80
c3. Max flux density in the stator yoke	T	≤ 1.80	≤ 1.80
c4. Linear current density (rms)	A/cm	≤ 400	≤ 400
c5. Efficiency @ base speed	%	≥ 90	≥ 90
c6. Maximum speed	rpm	≥ 20000	≥ 6000
c7. Back EMF @ maximum speed	V	≤ 120	≤ 40

The design optimization needs to satisfy several constraints to guarantee the reliability and feasibility of the final design. The considered constraints are listed in Table IV.

The flux density value in the stator yoke is slightly higher than the typical values [25], but for the proposed applications it is reasonable thanks to the use of high permeability core material.

The efficiency has been calculated as ratio between the output power and the output power plus the total losses.

The optimization have been carried out by imposing a constant value of the current vector, 30 A for the design M1 and 90 A for the design M2. By a preliminary analysis, the demagnetization of the magnets has been checked at the same negative direct current values with a PM minimum thickness of 2.0 mm.

The quantities fixed during optimization are shown in Table V.

The magneto-static Finite Element analysis is used to evaluate the motor performance and the design requirements (at base speed and maximum speed), namely to compute the objective function values and constraints of the minimization problem which represents mathematically the optimal design problem. The optimization procedure uses the information obtained by the FE program to iteratively update the set of motor parameters and try to identify an "optimal" motor by making a trade-off between the different parameters of the machine.

TABLE V
CONSTANT QUANTITIES

		M1	M2
air gap length	mm	0.5	0.4
inner rotor diameter D_{ir}	mm	50	24
outer stator diameter	mm	-	130

IV. THE OPTIMIZATION ALGORITHM

As described before, the optimal design problem of an IPM synchronous motor can be formulated as a particular multiobjective mixed-integer nonlinear programming problem. Its main features are the following:

- there are multiple objective functions that are conflicting with each other; it means that an improvement of one of them brings along a worsening of at least one of the others;
- some of the variables of the problem vary in a discrete way with fixed steps and this implies that the ratio between these variables and their steps must assume integer values.

In this paper authors focus in defining an algorithm which efficiently tackles the mixed integer aspect of the problem since it appears to be crucial for the considered design problem.

As regards the multiobjective aspect of the optimization problem, author's experience showed that, for this particular optimal design problem, a good compromise among different objectives can be obtained just by minimizing the sum of the weight of the motor and the opposites of the two torques.

Therefore the general structure of the considered optimization problem is the following:

$$\begin{aligned} &min\ f(x) \\ s.t.\ \ &g(x) \le 0 \\ &l \le x \le u \\ &x_i \in Z,\ i \in I_z \end{aligned} \qquad 4)$$

where Z is the set of the integer numbers, $x \in R^n$, $f: R^n \to R$, $g: R^n \to R^m$, $l, u \in R^n$, $l_i, u_i \in Z$, $i \in I_z$.

The set

$$F = \{ x \in R^n : g(x) \le 0,\quad l \le x \le u \}$$

is called feasible set.

However, a motor design problem has the following further distinguishing features that make it hard to be solved:

- the optimization problem may have different local minimum points besides the global one;
- an explicit mathematical representation of the objective function and of the constraint functions is not available, therefore the first-order derivatives of f and g_i cannot be

explicitly calculated or approximated;

- the objective function may not be available or defined when the point is unfeasible (i.e. the point do not satisfy the constraints);
- the constraints are highly non-linear and tight, an initial feasible design is not known and/or it is difficult to find a feasible point and to keep feasibility once it has been gained.

Authors decided to tackle the feasibility issue by means of an exact penalization of the constraints [27], [28]. Roughly speaking, the non-linearly constrained problem is converted into a box constrained one by adding to the objective function a term which penalizes the nonlinear constraint violations, that is "the augmented objective function",

$$P(x) = f(x) + 1/\varepsilon \max\{0, g_1(x), \ldots, g_m(x)\}.$$

where $\varepsilon = 10^{-1}$ is the penalty parameter.

Then, the following mixed integer box constrained problem is considered:

$$\begin{aligned} &\min\ P(x) \\ &s.t.\ \ l \le x \le u \\ &x_i \in Z,\ i \in I_z \end{aligned} \qquad 5)$$

In order to efficiently solve problem (5), a new algorithm belonging to the class of Controlled Random Search (CRS) algorithms has been proposed. This class derives from the original algorithm described in [29] and it has been proven to be useful and effective in solving several global optimization problems deriving from real world applications [30]-[33]. Similarly to other global optimization methods, CRS algorithms follow a strategy which combines a global search phase and a local search phase. The global search is used to locate the sub-regions "more promising" to contain a global minimizer; the local search is used for determining the global minimizer as soon as a "sufficiently small" neighborhood of this point has been located.

The basic idea of CRS methods is that of randomly generating an initial set of points in the box $l \le x \le u$ and iteratively updating this sample by substituting the worst point, in terms of objective function value, with a better one obtained by a local search. In this way the set of sample points should cluster more and more round the sub-regions which are more likely to contain a global minimizer. Therefore, these methods follow an approach which can be considered a compromise between a pure random search strategy and a clustering strategy derived by a deterministic local search.

In order to solve the mixed integer non linear programming problem (5), authors propose a modification of the algorithm proposed in [23] which directly handles the discrete variables with a reasonable computational effort.

Optimization Algorithm (OA)

Data: **Set** $m = 25\,n$ and $k = 0$
where n is the number of variables, m *is* the number of points in S^k and k is the iteration index.

Step 0: **Determine** $S^k = \{x_1^k, \ldots\ldots x_m^k\}$ a set of points chosen at random over $l \le x \le u$ and

Compute $P(x_{\max}^k) = \max_{x \in S^k} P(x)$
and $P(x_{\min}^k) = \min_{x \in S^k} P(x)$.

While *(stopping criterion* is not satisfied *)* **do**
Choose n+1 points over S^k with a *weighted random procedure* and rename these points as:

$x_{i_1}^k, \ldots, x_{i_n}^k, x_{i_{n+1}}^k$
with $P(x_{i_{n+1}}^k) \ge P(x_{i_j}^k),\ j = 1, \ldots, n.$

Compute the trial point $\tilde{x}^k$ by

$$\tilde{x}^k = c^k - \alpha^k\left(x_{i_{n+1}}^k - c^k\right)$$

where

$$c^k = \sum_{j=1}^{n+1} w_j^k x_{i_j}^k$$

$$\alpha^k = 1 - \frac{P(x_{i_{n+1}}^k) - \sum_{j=1}^{n+1} w_j^k\, P(x_{i_j}^k)}{P(x_{\max}^k) - P(x_{\min}^k) + \phi^k}$$

with

$$w_j^k = \frac{\eta_j^k}{\sum_{j=1}^{n+1} \eta_j^k},$$

$$\eta_j^k = \frac{1}{P(x_{i_j}^k) - P(x_{\min}^k) + \phi^k},$$

$$\phi^k = 10^3 \frac{(P(x_{\max}^k) - P(x_{\min}^k))^2}{P(x_{\max}^0) - P(x_{\min}^0)}$$

Discretize each variable $(\tilde{x}^k)_d$ whose index d belongs to the set I_z:

$$(\tilde{x}^k)_d = \left\lfloor \frac{(\tilde{x}^k)_d}{s_d} + \frac{1}{2} \right\rfloor s_d, \quad d \in I_z$$

where s_d is the step of the variable $(x)_d$.

If $\tilde{x}^k \in F$ and $f(\tilde{x}^k) \le f_{\max}^k$
then
Set $S^{k+1} = S^k \bigcup \{\tilde{x}^k\} \setminus \{x_{\max}^k\}$
Determine $P(x_{\max}^{k+1}) = \max_{x \in S^{k+1}} P(x)$ and
$P(x_{\min}^{k+1}) = \min_{x \in S^{k+1}} P(x)$.
Else
Set $S^{k+1} = S^k$, $x_{\min}^{k+1} = x_{\min}^k$, $x_{\max}^{k+1} = x_{\max}^k$
End if
Set $k = k + 1$
End while

The description of the algorithm is completed by the following procedures which specify the *weighted random*

procedure for determining $n + 1$ points over the set S^k and the *stopping criterion* for terminating the algorithm.

Weighted Random Procedure

Data: A set $S^k = \{x_1^k, ..., x_m^k\}$ such that

$P(x_i^k) \le P(x_{i+1}^k), i = 1, ..., m-1.$

For *j := 1, ...,n+1* **do**

Repeat:

generate a random number r_j uniformly distributed in [0,1] and compute $i_j = (2^{r_j} - 1)m$

Until $i_j \neq i_l, l = 1, ..., j-1$

End for

Select the set $\{x_{i_1}^k, ... x_{i_n}^k, x_{i_{n+1}}^k\}$ such that the point $x_{i_j}^k, j = 1, ..., n+1$, is the i_j –th element of the set S^k.

Stopping criterion

Data: A set $S^k = \{x_1^k, ..., x_m^k\}$ such that

$P(x_i^k) \le P(x_{i+1}^k), i = 1, ..., m-1,$ and set $\tilde{m} = 10n$.

If $\left(P(x_{\tilde{m}}^k) - P(x_1^k)\right) / P(x_1^k) \le 10^{-4}$

***Stop*.**

V. Comments to the Optimization Algorithm

The algorithm produces a sequence S^k of sets of m points. Initially (k=0), the set S^k is chosen at random on the set $l \le x \le u$ and then it is iteratively updated so as to include points which are better estimates of the global minimizers. In particular, at each iteration, the algorithm tries to "improve" the set S^k by replacing the point of the set S^k corresponding to the biggest function value with a new point where the objective function value is improved. The search of such a point is performed by using the information contained in the set S^k, in particular:

a) $n + 1$ points are chosen over the set S^k by using a weighted random procedure which privileges the points corresponding to smaller objective function values;

b) among these points, the point $x_{i_{n+1}}^k$ with the biggest function value is selected ;

c) the weighted centroid c^k of the selected $n + 1$ points $x_{i_1}^k$, …, $x_{i_n}^k$ $x_{i_{n+1}}^k$ is computed;

d) the new trial point $\tilde{x}^k$ is obtained by performing a suitable movement from c^k along the direction $c^k - \tilde{x}_{i_{n+1}}^k$.

The strategy to compute the point $\tilde{x}^k$ is based on the idea that the function values computed at the selected $n + 1$ points should give a good representation of the local behavior of the objective function around the point c^k. Therefore, in the point c^k, the vector $c^k - x_{i_{n+1}}^k$ should identify a good descent direction of the objective function, namely a direction along which the function should decrease, at least locally.

Detailed discussion and description of the formulae which define the weights w_j^k, j = 1, …, n + 1

and the step size α^k

in the weighted reflection are in [23], [30] and [31]. Here it is good to recall that, at the initial iterations

(when $\phi^k >> f(x_{i_j}^k) - f_{\min,}^k$

$w_{j,}^k \approx 1/(n+1),\ j = 1, \ldots,\ n+1$

and $\alpha^k \approx 1$),

these formulae are such that the weighted centroids and the new trial point are produced without privileging any particular point x_{i1}^k, …, $x_{i_{n+1}}^k$. As the number of iterations increases the centroid is defined by weighting more and more the points with smaller function values and the trial point is produced closer and closer to such points.

Finally, we note that the proposed algorithm does not need a (feasible) starting point. It produces a sequence S^k of sets of points starting from an initial set S^0. The points of S^0 are usually chosen at random on the set $l \le x \le u$. However, if one or more interesting points are known, the algorithm can exploit this information by including these points in the initial set S^0.

VI. Results

The proposed approach has been employed for the design optimization of two IPM synchronous motors in order to maximize the torque at base and high speed, extending the flux weakening region, minimizing the motor weight and satisfying a set of constraints. No initial feasible designs were requested because the optimization procedure does not need to start from a known initial design.

The Optimization Algorithm has been implemented in Fortran 90. The Finite Element analysis has been performed by ANSYS® Rev. 11. All the numerical results have been obtained on an Intel Core2 duo CPU 2.66GHz with 1,96GB main memory.

A. Design M1

Main data and simulation results of the optimized design are presented in Table VI: it includes some of the key machine dimensions and performance at base and maximum speed.

Cross-section of the optimized design is provided in Fig. 5. The optimization required about 13000 objective function calls by FE analysis: for each call, two operating points have been tested (at base speed and maximum speed).

Figures 6 and 7 show the trend of the augmented objective function *P(x)* (sum of the weight of the motor and the opposites of the two torques) and the single objective functions vs. iterations.

The accurate motor design optimization has allowed to

maximize the torque keeping down the weight of active materials without oversizing the machine. The slot fill factor value is very close to the boundary and it guarantees the feasibility of the stator windings. At base speed (4000 rpm), the efficiency is satisfactory exceeding 90% and the torque is higher than 12 Nm. In the flux weakening operation, the optimized design presents a torque of 2.4 Nm at the maximum speed of 24000 rpm. The back EMF is widely satisfied. Maximum flux densities in the stator tooth and stator yoke are 1.74 T and 1.80 T.

TABLE VI
OPTIMIZED DESIGN M1

Stack length	82	mm
Outer stator diameter	118	mm
Inner stator diameter	76.2	mm
PM thickness	2.10	mm
Magnet position	5.81	mm
Ratio of PM width to barrier width	0.89	
Thickness of steel bridge	2.0	mm
Number of wires per slot	12	
Wire size	1.75	mm
Stator slot fill factor	0.377	
Iron gross Weight	7.0	kg
Copper Weight	1.88	kg
PM Weight	0.19	kg
Phase current (peak value)	30.0	A
Linear current density (rms)	361	A/cm
Base speed	4000	rpm
Efficiency @ base speed	92.0	%
Torque @ base speed	12.3	N·m
Output power @ base speed	5151	W
Maximum speed	24000	rpm
Torque @ max. speed	2.4	N·m
Output power @ max. speed	6031	W
Losses per radiating slot surface	10.4	W/dm^2

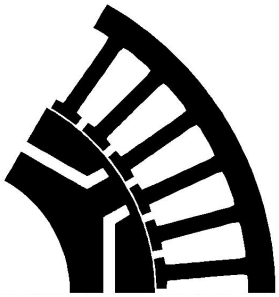

Fig. 5. Stator and rotor shape (1 pole) of the optimized design M1.

Thermal performance has been checked by introducing the specific losses, i.e. losses per radiating slot surface:

$$L_S = \frac{\rho k_r w_s \sigma^2}{2\left(\frac{w_s}{h_s}+1\right)}$$

where σ is the current density, k_s the stator slot fill factor, ρ the copper resistivity (at reference temperature of 90°C), w_s the average slot width and h_s the slot high.

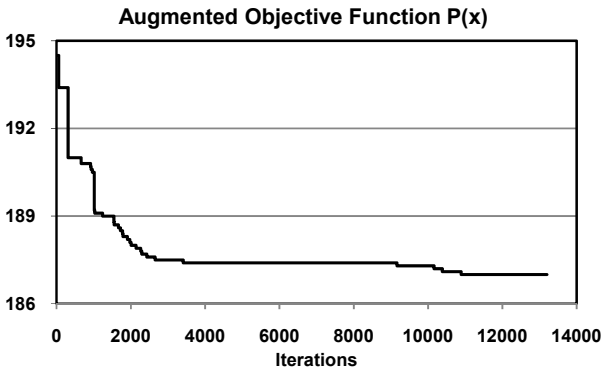

Fig. 6. Design M1. Progress of the augmented objective function vs. iterations.

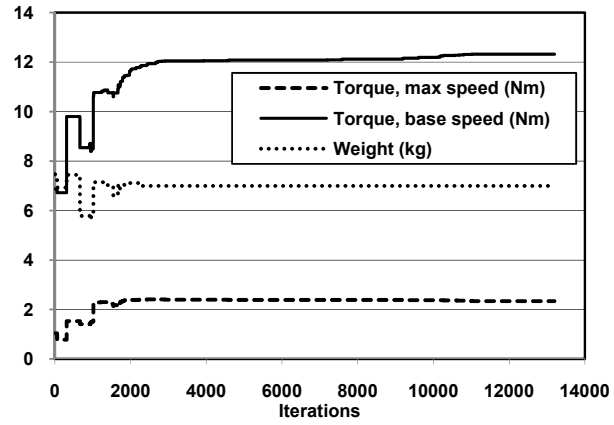

Fig. 7. Design M1. Progress of the single objective functions vs. iterations.

In motor M1, losses per radiating slot surface are 10.4 W/dm^2 and assure good machine thermal performance.

Figures 8 and 9 show the calculated torque-vs-speed and output power-vs-speed characteristics from FE analyses, by imposing the current trajectory (current circle) described in Section II.

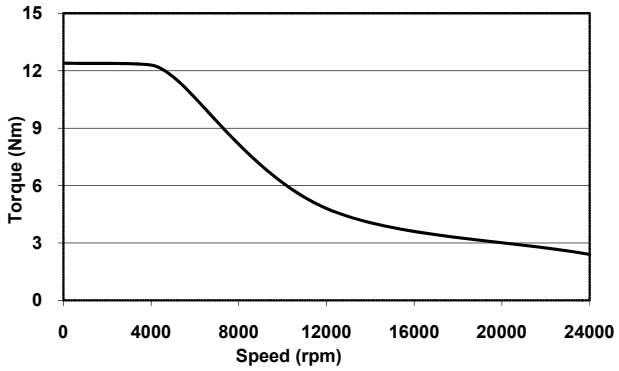

Fig. 8. Design M1. Calculated torque vs. speed characteristic.

The motor has excellent field-weakening performance: it is evident how the constant-power speed range is wide and the goal of our study has been fully satisfied.

Figures 10 and 11 show the FE calculated variation of the *d-axis* and *q-axis* fluxes for different values of i_d and i_q.

Fig. 10 points out the nearly linear effect of the *d-axis* current and the cross-saturation effect due to *q-axis* current, decreasing with increasing demagnetizing *d-axis* current.

Fig. 11 shows the non linear effect of the *q-axis* current on the *q-axis* flux and the limited cross-saturation effect due to the *d-axis* current.

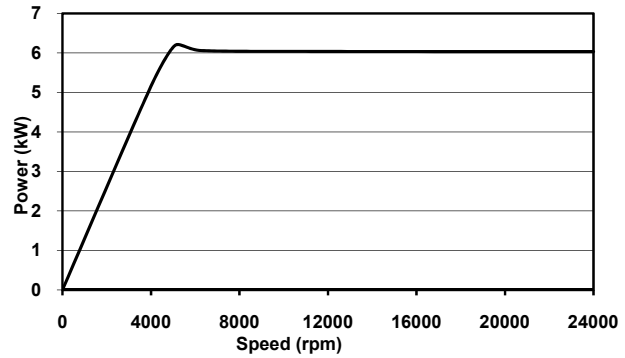

Fig. 9. Design M1. Calculated output power vs. speed characteristic.

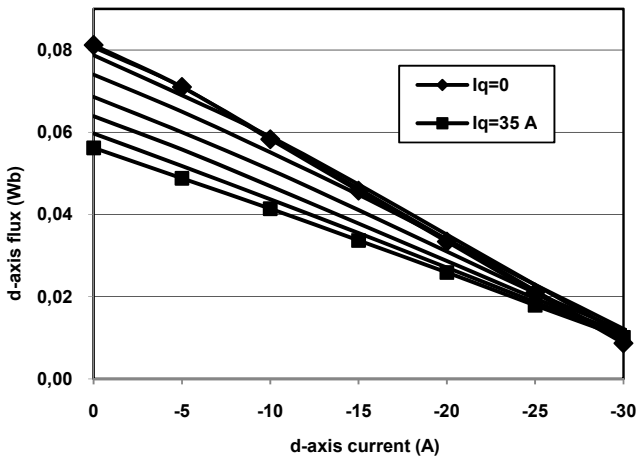

Fig. 10. Design M1. *d*-axis flux vs *d*-current at different *q*-current.

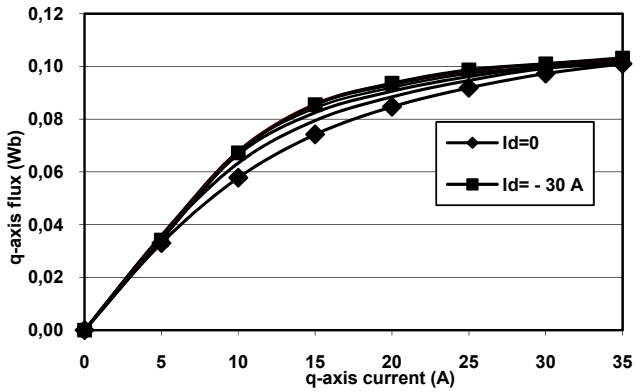

Fig. 11. Design M1. *q*-axis flux vs *q*-current at different *d*-current.

B. *Design M2*

Main data and simulation results of the motor are presented in Table VII. It includes some of the key machine dimensions and the performance at base and maximum speed: at base speed (2600 rpm) the rated torque is 17 Nm and the efficiency is 91%. The obtained maximum speed is 8000 rpm (constraint at 6000 rpm) where the torque is 6.3 Nm. Maximum flux density in the teeth and in the yoke do not exceed 1.7 T, whereas it is about 1.5 T in the rotor tooth. Thermal performance are guaranteed by the low value of losses per radiating slot surface (8.3 W/dm^2).

The optimization required about 12000 objective function calls by FE analysis.

Based on the optimized design, a prototype has been realized (Fig. 12): rotor lamination of the optimized design is shown in Fig. 13.

TABLE VII
Optimized design M2

Stack length	115	mm
Inner PM thickness	5.0	mm
Outer PM thickness	2.3	mm
Inner PM position	9.2	mm
Thickness of steel bridge	1.2	mm
Number of wires per slot	3	
Wire size	3.10	mm
Stator slot fill factor	0.392	
Iron gross Weight	12.0	kg
Copper Weight	2.03	kg
PM Weight	0.51	kg
Phase current (peak value)	90.0	A
Linear current density (rms)	260	A/cm
Base speed	2600	rpm
Efficiency @ base speed	91.0	%
Torque @ base speed	17.0	Nm
Output power @ base speed	4628	W
Maximum speed	8000	rpm
Torque @ max. speed	6.3	Nm
Output power @ max. speed	5278	W
Losses per radiating slot surface	8.3	W/dm^2

Fig. 14 shows the experimental set-up used to characterize the performance of the manufactured prototype and verify the design optimization. It includes the IPM prototype, a current-regulated (CR) vector controlled drive and a brake. The motor is speed controlled through a proportional-integral (PI) controller. The output of the speed controller works as the *q*-current (torque) reference, while the *d*-current reference can be freely imposed by the user. The brake allows setting the value of the load torque (T_l) in each test, while a digital wattmeter (DW) allows for the measurement of phase currents, voltages and input power. The basic goal of the characterization has been the evaluation of the *d-q* currents along the voltage limit ellipses at different speed at flux-weakening, e.g. curve YZ in Fig. 15.

The procedure starts by setting the reference speed with *d* current reference at zero. Increasing the load, the action of the speed regulator increases the (torque) *q*-current until the voltage reach the maximum (point Y). By setting a proper step of variation for the *d* current and load, the subsequent operating points track the voltage limit ellipse as shown in the

Figure 15. At point Z the maximum torque is achieved at maximum current and voltage. Such "increasing load" tests, repeated all over the flux-weakening region, allow to identify the motor performance at constant current (current circle) and at maximum voltage (voltage limit ellipses). Fig. 15 shows the experimental operating points along the voltage ellipses at 3000 and 6000 rpm.

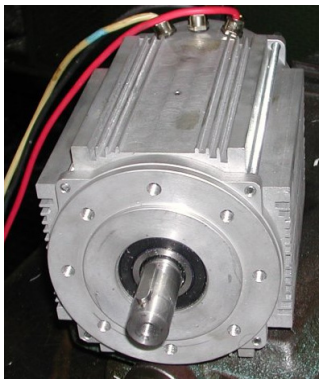

Fig. 12. Design M2. View of the prototype.

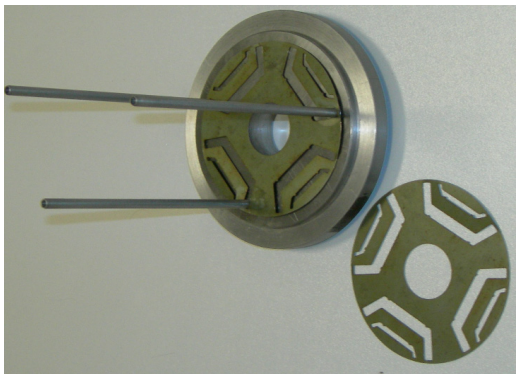

Fig. 13. Design M2. Rotor lamination.

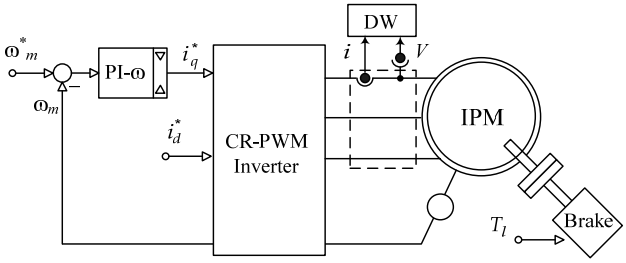

Fig. 14. Set-up for experimental characterization.

Operating points on current circle at variable speed are reported in Figures from 16 to 19, as torque, output power, *d,q*-currents and efficiency (direct method) vs. speed, in comparison with the simulation results.

They confirm the reliability of the simulation results and the effectiveness, the versatility and the robustness of the proposed procedure.

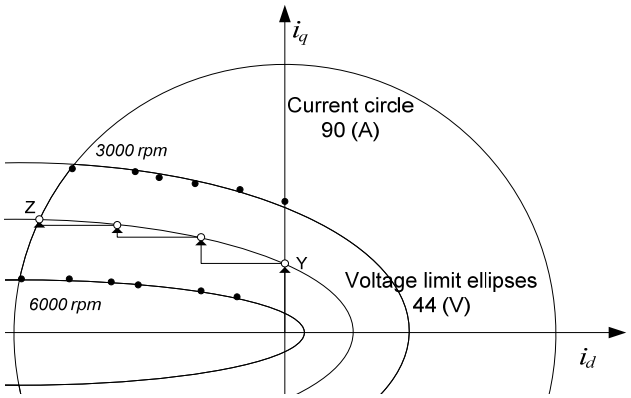

Fig. 15. Design M2. Evaluation of the *d-q* currents along voltage limit ellipses at different speed at flux-weakening. Experimental results at 3000 and 6000 rpm.

VII. Conclusions

Authors propose a procedure to design IPM synchronous motors with minimum weight, maximum output power and suitable for wide constant-power region operation. The design problem has the following main features:

- complex rotor geometry with high magnetic nonlinearity;
- design concerns all the motor dimensions (stator and rotor core, winding and magnets);
- design is evaluated in two distinct operating points (rated and high speed);
- several continuous and discrete variables;
- several, highly non-linear and tight constraints;
- multiple objectives, one term conflicting with the others;
- objective and constraint functions cannot be explicitly calculated or approximated;
- different local minimum points besides the global one;
- initial feasible design could be not known and it is difficult to keep feasibility once it has been gained.

It has been formulated as a particular multiobjective mixed-integer nonlinear programming problem. The multiobjective aspect of the optimization problem has been approached minimizing the sum of the conflicting objectives, whereas the feasibility issue has been tackled by means of an exact penalization of the constraints, that is adding to the objective function a term which penalizes the nonlinear constraint violation.

The design problem has been solved by the use of a new algorithm proposed by the authors. It belongs to the class of Controlled Random Search (CRS) algorithms and directly handles the discrete variables with reasonable computational effort.

The algorithm does not need a (feasible) starting point and combines a global search phase and a local search phase.

The remarkable saturation phenomena due to the buried magnets in the rotor have been taken into account by Finite Element analysis which has been used to evaluate all motor performance.

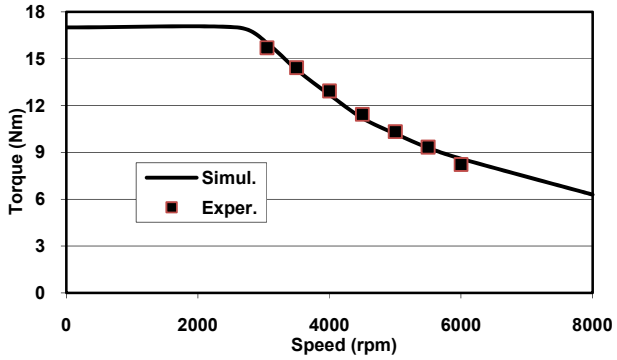

Fig. 16. Design M2. Comparisons between FE simulated and experimental torque vs. speed characteristics.

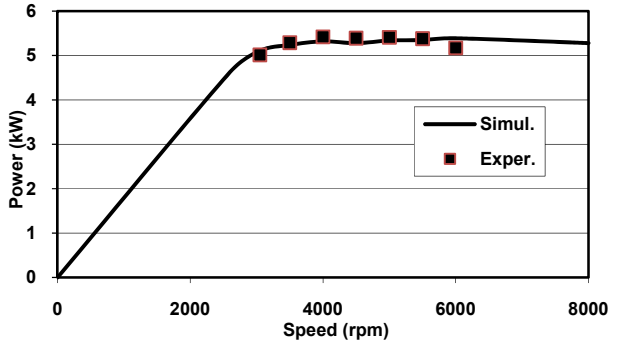

Fig. 17. Design M2. Comparisons between FE simulated and experimental output power vs. speed characteristics.

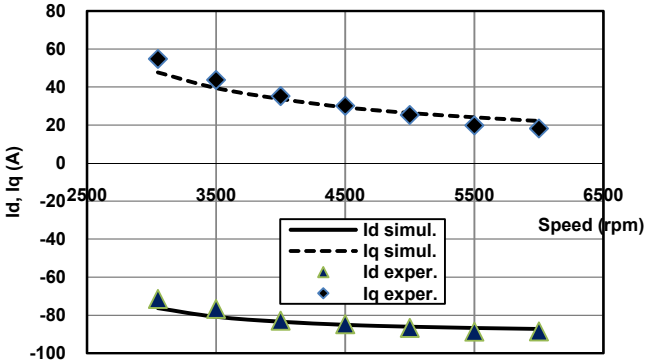

Fig. 18. Design M2. Comparisons between FE simulated and experimental *d-q* currents vs. speed characteristics.

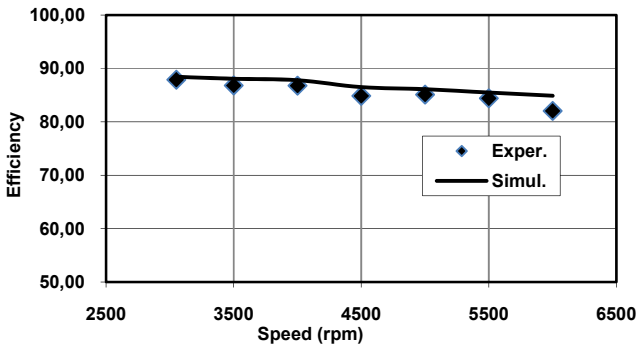

Fig. 19. Design M2. Comparisons between FE simulated and experimental efficiency vs. speed characteristics.

To test the proposed optimization procedure two case studies have been considered: the design of an IPM motor for industrial application and the design of an IPM motor for city electrical scooter. In the examples of application, authors decided to consider two cases without initial design availability; hence it is not possible to compare the final with the initial designs; that is not a lack of the procedure, but one of its peculiarity.

In conclusion, the results reported in this work show the importance of using optimization procedures in the context of motor design. In fact, even if the considered optimization problem is a global one and the final designs can not be defined the "best" ones, the proposed method appears to be quite interesting anyway. From a mathematical point of view, the final designs guarantee the satisfaction of the constraints in the model and represent a good solution in terms of objective function value. The examples of application and the prototype demonstrate that optimization and simulation results are reliable and confirm, indirectly, the procedure.

REFERENCES

[1] A. Guerriero, F. Parasiliti, M. Tursini, "Optimum Vector Control of High Efficiency Interior PM Synchronous Motor", in *Proc. of Energy Efficiency in Motor Driven Systems Conference (EEMODS'07),* June 2007.

[2] Shinn-Ming Sue, Ching-Tsai Pan, "Voltage-Constraint-Tracking-Based Field-Weakening Control of IPM Synchronous Motor Drives," *IEEE Trans. on Industrial Electronics,* vol. 55, no. 1, pp. 340-347, Jan 2008.

[3] M. Nasir Uddin, M. Azizur Rahman, "High-Speed Control of IPMSM Drives Using Improved Fuzzy Logic Algorithms," *IEEE Trans. on Industrial Electronics,* vol. 54, no. 1, pp. 190-199, Feb 2007.

[4] B. Cheng, T. R. Tesch, "Torque Feedforward Control Technique for Permanent-Magnet Synchronous Mot," *IEEE Trans. on Industrial Electronics*, vol. 57, no. 3, pp. 969-974, March 2010.

[5] Cheol Jo, Ji-Yun Seol, In-Joong Ha, "Flux-Weakening Control of IPM Motors With Significant Effect of Magnetic Saturation and Stator Resistance," *IEEE Trans. on Industrial Electronics,* vol. 55, no. 3, pp. 1330-1340, March 2008.

[6] F. Parasiliti, R. Petrella and M. Tursini, "Speed Sensorless Control of an Interior PM Synchronous Motor", in *Proc. 2002 IEEE Industry Applications Conference* – Pittsburgh, Pennsylvania, USA, October 13 18, 2002.

[7] Sung-Yeol Kim, In-Joong Ha, "A New Observer Design Method for HF Signal Injection Sensorless Control of IPMSMs," *IEEE Trans. on Industrial Electronics,* vol. 55, no. 6, pp. 2525-2529, June 2008.

[8] G. Foo, M. F. Rahman, "Sensorless Direct Torque and Flux-Controlled IPM Synchronous Motor Drive at Very Low Speed Without Signal Inject," *IEEE Trans. on Industrial Electronics,* vol. 57, no. 1, pp. 395-403, Jan 2010.

[9] F. Parasiliti, P. Poffet, "A Model for Saturation Effects in High-field Permanent Magnet Synchronous Motors", *IEEE Transactions on Energy Conversion*, vol. 4, no. 3, pp. 487-494, September 1989.

[10] L. Parsa, Lei Hao, "Interior Permanent Magnet Motors With Reduced Torque Pulsation," *IEEE Trans. on Industrial Electronics,* vol. 55, no. 2, pp. 602-609, Feb 2008.

[11] Jin Hur, "Characteristic Analysis of Interior Permanent-Magnet Synchronous Motor in Electrohydraulic Power Steering Systems," *IEEE Trans. on Industrial Electronics,* vol. 55, no. 6, pp. 2316-2323, June 2008.

[12] P. E. Kakosimos, A.G. Kladas, "Modeling of interior permanent magnet machine using combined field-circuit analysis", in *Proc. of 2010 International Conference on Electrical Machines (ICEM 2010).*

[13] K. Yamazaki, H. Ishigami, "Rotor-Shape Optimization of Interior-Permanent-Magnet Motors to Reduce Harmonic Iron Los," *IEEE Trans. on Industrial Electronics,* vol. 57, no. 1, pp. 61-69, Jan 2010.

[14] D. Iles-Klumpner, M. Risticevic, I. Boldea, "Advanced Optimization Design Techniques for Automotive Interior Permanent Magnet Synchronous Machines", *2005 IEEE International Conference on Electric Machines and Drives*, pp. 227-234.
[15] D. Iles-Klumpner, I. Boldea, "Comparative optimization design of an interior permanent magnet synchronous motor for an automotive active steering system", in *Proc. of the 35th Annual IEEE Power Electronics Specialists Conference*, Aachen, Germany, 2004, pp. 369-375.
[16] Sang-Ho Lee, Jung-Pyo Hong, Sang-Moon Hwang, Woo-Taik Lee, Ji-Young Lee, Young-Kyoun Kim, "Optimal Design for Noise Reduction in Interior Permanent-Magnet Motor", *IEEE Trans. on Industry Applications*, vol. 45 , pp. 1954 – 1960, 2009.
[17] Jeonghu Kwack, Seungjae Min, Jung-Pyo Hong, "Optimal Stator Design of Interior Permanent Magnet Motor to Reduce Torque Ripple Using the Level Set Method", *IEEE Trans. on Magnetics*, vol. 46 , pp. 2108 - 2111, 2010.
[18] Shanshan Wu; D.D. Reigosa, Y. Shibukawa, M.A. Leetmaa, R.D. Lorenz, Yongdong Li, "Interior Permanent-Magnet Synchronous Motor Design for Improving Self-Sensing Performance at Very Low Speed", *IEEE Trans. on Industry Applications*, vol. 45 , pp. 1939 – 1946, 2009.
[19] P. Sergeant, F. De Belie, J. Melkebeek, "Rotor geometry design of an interior permanent-magnet synchronous machine for more accurate sensorless control", in *Proc. of 2010 International Conference on Electrical Machines (ICEM 2010)*.
[20] X. Jannot, J.-C. Vannier, C. Marchand, M. Gabsi, J. Saint-Michel, D. Sadarnac, "Multiphysic Modeling of a High-Speed Interior Permanent-Magnet Synchronous Machine for a Multiobjective Optimal Design" *IEEE Trans. on Energy Conversion*, vol. PP, pp. 1 – 11, 2011.
[21] M. Barcaro, N. Bianchi, F. Magnussen, "Design considerations to maximize performance of an IPM motor for a wide flux-weakening region", in *Proc. of 2010 International Conference on Electrical Machines (ICEM 2010)*.
[22] G. Pellegrino, F. Cupertino, "IPM motor rotor design by means of FEA-based multi-objective optimization", in *Proc. of 2010 IEEE International Symposium on Industrial Electronics (ISIE 2010),* pp. 1340 – 1346.
[23] G. Liuzzi, S. Lucidi, F. Parasiliti, M. Villani, "Multi-objective Optimization Techniques for the Design of Induction Motors"*, IEEE Transactions on Magnetics*, vol. 39, n.3, pp. 1261-1264, 2003.
[24] W.L.Soong, S.Han, T.M. Jahns, "Design of Interior PM Machine for field-weakening Applications", in *Proc. of. Int. Conf. on Electrical Machines and Systems*, October 8-11, 2007, pp. 657-664.
[25] D. Zarko, D. Ban, T. A. Lipo, "Design Optimization of Interior Permanent Magnet Motor with Maximum Torque Output in the Entire Speed Range", in *Proc. Int. Conf. On Power Electronics and Applications 2005*, Dresden.
[26] J. F. Gieras, M. Wing, *Permanent Magnet Motor Technology,* New York: Marcel Dekker Inc., 2002.
[27] W. I. Zangwill, "Nonlinear Programming via Penalty Functions", *Management Science*, 13 pp. 344-358, 1967.
[28] G. Di Pillo and L. Grippo, "On the exactness of a class of Non-differentiable penalty Functions", *Journal of Optimization Theory and Applications*, 57, no. 3, pp. 399-410, 1988.
[29] W. L. Price, "Global optimization by controlled random search", *Journal of Optimization Theory and Applications*, 40 (1983), 333-348.
[30] P. Brachetti, M. De Felice Ciccoli, G. Di Pillo, and S. Lucidi, "A new version of the Price's algorithm for global optimization", *Journal of Global Optimization*, 10 (1997), 165-184.
[31] W. L. Price., "Global optimization algorithms for a CAD workstation", *Journal of Optimization Theory and Applications*, 55 (1987), 133-146.
[32] A. Daidone, F. Parasiliti, M. Villani, S. Lucidi, "A New Method for the Design Optimization of Three-Phase Induction Motors", *IEEE Transaction on Magnetics*, vol. 34, n. 5, pp. 2932-2935, 1998.
[33] F. Parasiliti, M. Villani, S. Lucidi, F. Rinaldi, "A new optimization approach for the design of IPM synchronous motor with wide constant-power region", in *Proc. of 2010 International Conference on Electrical Machines (ICEM 2010)*.

Francesco Parasiliti was born in Tortorici, Italy, in 1956. He received the M.S. degree in electrical engineering from the University of Rome, Italy, in 1981. In 1983 he joined the Department of Electrical Engineering of the University of L'Aquila, Italy, as an Assistant Professor. From 1987 to 1988 he worked as Research Fellow at the Swiss Federal Institute of Technology of Lausanne (Switzerland). From 1992 to 1999 he has been an Associate Professor of Electrical Drives at the University of L'Aquila. Since 2000 he is Full Professor at the same University. Currently he is member of the Steering Committee of the International Conference on Electrical Machines. He has published more than 120 papers in scientific journals and conference proceedings. His studies deal with design optimization of induction, permanent magnet synchronous and reluctance motors, modeling and parameter observation of induction and synchronous machines, digital control of electrical drives including vector, sensorless and fuzzy logic control.

Marco Villani was born in Lecce, Italy, in 1960. He received the M.S. degree in electrical engineering from the University of L'Aquila, L'Aquila, Italy, in 1985. He became an Assistant Professor of power converters, electrical machines, and drives in 1993. In 1990, he was Research Fellow at the University of Dresden, German, and in 1995 at the Nagasaki University, Nagasaki, Japan. In 1998 he cooperated in two EU-SAVE projects concerning the Energy efficiency improvements in three-phase induction motors. He is currently professor of Electrical Machines Design for the degree of Engineering at the University of L'Aquila. His research interests are focused on modeling and simulation of electrical machines, energy saving in electric motors, optimization techniques for the electrical machines design, design of PM synchronous motors and Reluctance motors. He is author of more than 90 technical papers in scientific journals and conference proceedings.

Stefano Lucidi received the M.S. degree in electronic engineering from the "Sapienza" University of Rome, Italy, in 1980. From 1982 to 1992 he was Researcher at the Istituto di Analisi e dei Sistemi e Informatica of the National Research Council of Italy. From September 1985 to May 1986 he was Honorary Fellow of the Mathematics Research Center,of University of Wisconsin, Madison, USA. From 1992 to 2000 he was Associate Professor of Operations Research of the "Sapienza" University of Rome. Since 2000 he is Full Professor of Operations Research of the "Sapienza" University of Rome. He teaches courses on Operations Research and Global Optimization methods in Engineering Management. He belongs to the Department of Computer and System Sciences of the "Sapienza" University of Rome. From November 2010, he is the Director of the PhD Programme in Operations Research of the "Sapienza" University of Rome. His research interests are mainly focused on the study , definition and application of nonlinear optimization methods and algorithms. This research activity has produced 72 papers published in international journals and 17 papers published in international books.

Francesco Rinaldi was born in Foggia, Italy, in 1980. He received the M.Sc. degree in computer engineering (summa cum laude) and the PhD degree in operations research from the "Sapienza" University of Rome in 2005 and 2009, respectively. He is currently a research fellow in the Department of Computer and System Sciences "A. Ruberti", at the "Sapienza" University of Rome. His research interests include nonlinear optimization, data mining and machine learning. He has published about 10 papers on international journals.